COMPDYN 2013
4th ECCOMAS Thematic Conference on
Computational Methods in Structural Dynamics and Earthquake Engineering
M. Papadrakakis, V. Papadopoulos, V. Plevris (eds.)
Kos Island, Greece, 12–14 June 2013

BALANCING THE BENEFICIAL CONTRIBUTIONS OF FOUNDATION ROCKING AND STRUCTURAL YIELDING TO IMPROVE STRUCTURAL SEISMIC RESILIENCE

Weian Liu[1], Tara C. Hutchinson[1], Bruce L. Kutter[2], Manouchehr Hakhamaneshi[2], and Andreas-Gerasimos Gavras[2]

[1] Department of Structural Engineering, University of California, San Diego, USA
9500 Gilman Drive, Mail Code 0085, La Jolla, CA, USA 92093-0085
e-mail: {wel007, tara}@ucsd.edu

[2] Department of Civil and Environmental Engineering, University of California, Davis, USA
2001 Ghausi Hall, 1 Shields Avenue, Department of Civil & Environmental Engineering, University of California, Davis, CA, USA 95616
{blkutter, mhakhamaneshi, aggavras}@ucdavis.edu

Keywords: Foundation Rocking, Structural Hinging, Seismic Performance.

Abstract. *To date, numerous individual and system-level experimental studies have illustrated that the mode of foundation rocking advantageously can provide dissipation of seismic energy and re-centering of a structural system. Likewise, within the framework of performance-based earthquake engineering, structural components are strategically designed to behave inelastically. Balancing the beneficial attributes of each of these yielding systems has the potential to increase seismic resilience of the foundation-building system.*

This paper considers a balanced design strategy whereby the strength of a rocking footing is equated to the strength of inelastic structural fuses within the superstructure of a building. This balanced design concept is applied to the design of two model-building structures constructed and tested on the large geotechnical centrifuge at the University of California, Davis. Model buildings included a 3-dimensional low-rise frame-type and a 2-dimensional wall-type structure supported on shallow footings, where footing sizes were sized to encourage inelastic rocking. Two extreme hinging dominated systems, namely, a Foundation Rocking Dominated (FRD) and Structural Hinging Dominated (SHD) system were simultaneously constructed and tested as well. Experiments show that for a balanced design frame-braced configuration, the energy is well distributed between structural and footing fuses. In wall-type foundation-building systems, the FRD system observes significantly larger total roof drift, much of which is accumulated at the foundation level. Irrespective of the structure type, base shear demand in is greatly minimized when footing rocking is initiated in both the balanced design and FRD model.

1 INTRODUCTION AND SCOPE

1.1 Introduction

During a traditional building or bridge design, an engineer usually assumes that the foundation is fixed, while the superstructure carries the deformation induced during static and dynamic loading. This design concept leads to two major consequences, namely: (1) a design with unreasonably oversized foundation components to support the "fixed" condition and (2) a design which constrains plastic hinging behavior to the above-ground structural elements during a seismic event, such as at the ends of beams or at the base of shear walls, within the structural wall itself. Nonetheless, allowing the foundation to uplift at the ends has been gradually acknowledged as an effective inelastic mode to dissipate dynamic input energy. Moreover, such a mode promotes a natural re-centering tendency of the structure with the aid of the so-called "P-Δ effect". Commonly in the literature this is referred to as the *foundation rocking mechanism*. Numerous foundation-level component tests uniformly verify the advantageous seismic benefits of this mechanism.

Often cited as the earliest, most convincing work identifying such a mechanism are the field observations documented by Housner [11], who conducted field reconnaissance following the 1960 Valdivia earthquake in Chile. He observed that several lollipop structures survived, while modern structures were severely damaged. Researchers in New Zealand in the 1970s (e.g. Bartlett [3] and Wiessing [22]) subsequently conducted a series of 1-g experiments on shallow foundation-shearwall systems with footings of various sizes and vertical factors of safety (*FSv*). These experiments provided highly convincing moment-rotation hysteresis at the footing level that further substantiated the merits of the rocking footing mechanism. More recently, researchers across the United States and Europe have undertaken a variety of 1-g and centrifuge tests coupled with numerical work to investigate the mobilization of soil-foundation capacity (see e.g. Rosebrook and Kutter [17]; Gajan and Kutter [8]; Anastasopoulos et al. [1]; Deng et al. [5]; Hakhamaneshi et al. [10]; Gelagoti et al. [9]; Drosos et al. [6]). Since the centrifuge facility has the capability to create confining stress levels comparable with prototype conditions, the stress-dependent soil nonlinear behavior can thereby be reasonably captured. A common strategy in centrifuge testing has involved placing a number of simple structural assemblies, such as a shearwall-footing system or a single degree-of-freedom (SDOF) lollipop structural model supported on a shallow foundation element and subjecting the models to combined compression (N-g) and cyclic inertial or ground excitation loading. Model foundations have been designed with various geometries, FS_v, and different types of soils. In general, centrifuge tests concur that irrespective of the soil type, footings with a relatively high FS_v (~10) will result in quite reasonable moment-rotation hysteresis, which quantifiably dissipates energy, without significant settlement (Deng et al. [5]; Hakhamaneshi et al. [10]). Large-scale 1-g tests on shallow footings report similar findings (e.g. Taylor and Crewe [19], Negro et al. [15], Paolucci et al. [16] and Shirato et al. [18]).

Given the demonstrated benefits of the rocking foundation component, the merits of integrating it into the overall soil-structure system need to be studied on level playing field with other inelastic mechanisms. To the authors' knowledge, only a handful of test programs have considered the dual inelastic mechanisms of soil and structural components. For example, Chang et al. [4] examined a set of 2-dimensional physical shearwall-frame building models considering the nonlinear behavior of the footings coupled with inelastic structural fuses within the superstructure. More recently, Deng et al. [5] incorporated the foundation rocking mechanism into a bridge structural system while also accounting for a common column hinging mechanism. Trombetta et al. [21] constructed and tested a pair of 3-dimensional inelastic frame models to study the effect of building adjacency on the seismic response.

1.2 Scope of this work

Although a handful of experiments have considered the participation of both foundation and structural components to a systems seismic resistance, prior test efforts did not strategically implement a targeted design strategy. To embrace the foundation rocking mechanism within a conventional structural design paradigm, it is useful to systematically consider the systems behavior with varying levels of foundation strength. In parallel, typical earthquake-resistant structural configurations within a building system incorporate structural fuse mechanisms within the superstructure components to dissipate seismic energy; therefore such a systematic study should similarly embrace this philosophy. The question of how these two inelastic components dynamically interact with each other and share the seismic demand is still unreported and warrants a future investigation. In a research program supported by National Science Foundation (NSF), we investigate the seismic performance of this integrated inelastic foundation-building system. In this paper, we propose balancing the demands to each of these components, and apply this methodology to the design of a series of centrifuge test models. Two different building configurations are constructed at centrifuge scale, namely a 3-dimensional frame-type structure and a 2-dimensional wall-type structure. Select experimental data for these two systems are presented and compared with other models, in which the yielding of structural fuse and rocking foundation is unbalanced.

2 BALANCED DESIGN METHODOLOGY

Within the framework of performance-based earthquake engineering, structural components are encouraged to behave inelastically. For instance, a weak-beam strong-column strategy is a common inelastic mechanism adopted in the seismic design of frame-braced buildings. This strategy aims to localize the plastic behavior at the ends of beam elements, therefore ensuring that damage to beams will occur prior to column failure. Columns provide essential support for transferring gravity loads in a building; therefore their failure could result in an undesired catastrophic building collapse. For a wall-based lateral load resisting system, even with frame elements integrated within the system, the shear wall component is designed to carry the majority of the lateral load. Consequently, the plastic hinging behavior will inevitably occur at the interface between the wall and footing. Figure 1a depicts a hysteresis for a structural wall fuse, and quite comparably broad and stable hysteresis can be realized at the footing-soil interface as well (Figure 1b).

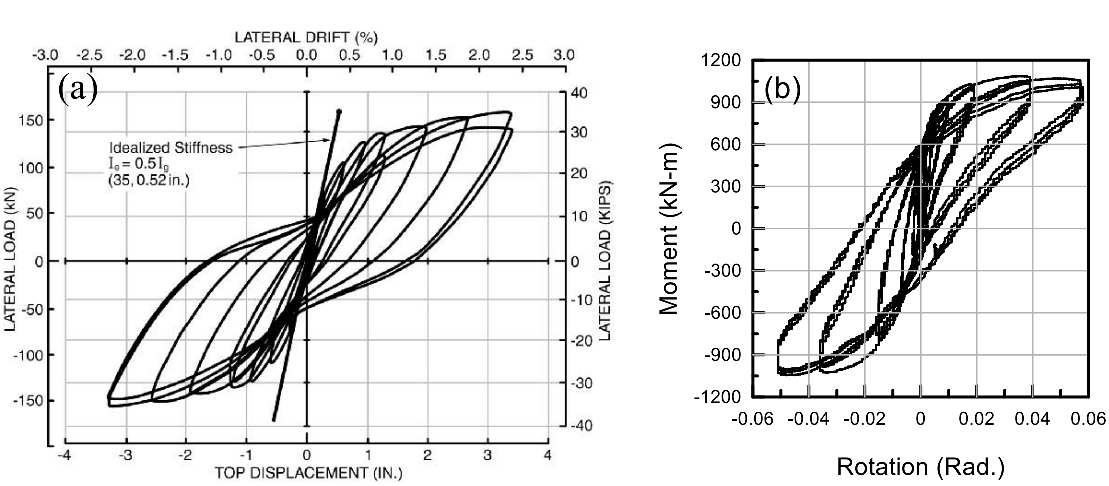

Figure 1: Hysteretic curves for concrete shear wall (test by Taylor et al. [20], adapted from Englekirk [7]) and rocking-dominated footing in prototype scale (Hakhamaneshi et al. [10]).

When the rocking footing mechanism is integrated into a building system, considering the strength difference between these two plastic behaviors, three fundamental systems could be realized. One extreme may be when the footing's load capacity is significantly larger than that of the structural fuse; the foundation component is intended to be protected during seismic events, while the structural fuse is expected to carry large inelastic demands. In this paper, we refer to this system as a **Structural Hinging Dominated** (SHD) system. Most of the existing buildings fall into this category. They are usually constructed with oversized foundations, which in turn increase the overall construction cost. If properly designed, this system could perform well during a design-level earthquake. On the other extreme, one could realize inelastic behavior solely via the mechanism of footing rocking. In this paper, we refer to this type of system as a **Foundation Rocking Dominated** (FRD) system. This is a theoretically proposed, yet unimplemented building configuration in reality. Nonetheless, the final behavior of a FRD building is akin to that observed when a building is base isolated (BI), namely nearly all shear strains are absorbed close the ground level. In contrast to the BI building, which would largely translate horizontally, an FRD building would rotate. The foundation geometry could be designed considerably smaller than an SHD system, however, superstructure components would need to be relatively strong, particularly within regions of the structure where large seismic forces cumulate (such as the ends of beams and columns). This type of system has the potential to reduce the residual displacement on the superstructure due to its inherent re-centering characteristic. However, depending on the soil stiffness, large amplitude rocking at the footing-soil interface could potentially exacerbate footing absolute or differential settlement. Adopting the beneficial attributes of both superstructure and foundation fuses by equating the strengths of both components is appealing, and in this paper we term this a **Balanced Design** (BD) system. Ultimately, some type of optimization should be considered and perhaps this does not stem from equitable strength distributions, but more careful consideration of the kinematics of the building as a system. We hypothesize that the balanced design system however provides an initial compromise to demonstrate avoidance of extreme behaviors, such as significant story drift or excessive foundation settlement. Compared with the SHD system, this configuration could not only save construction cost for foundations, but also continue to maintain the self-centering benefits of an FRD system.

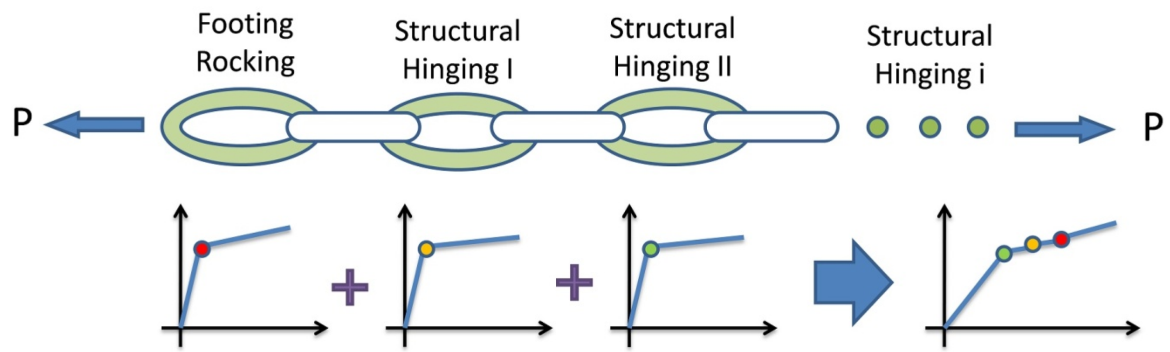

Figure 2: Illustrative Chain Analogy.

To emphasize the fundamental concept of a balanced design philosophy, a chain analogy is illustrated as shown in Figure 2. In this figure, each chain element represents a ductile component in the entire building-footing system. Footing rocking behavior certainly plays an important role in seismic energy dissipation, and thereby serves as a fundamental ductile link within the chain. In a complex structural system, structural hinging behavior is not always limited within one or two elements; therefore, it usually develops a multi-fuse mechanism during seismic activities. When the entire system is subjected to an external force P, the link with the weakest capacity is the first element to develop nonlinear behavior. Consequently, the potential contributions from other stronger links will be limited and the system global behavior will be solely governed by the weakest part in this idealized series system. However, when all the inelastic elements are prone to yield under the same P, as illustrated in Figure 2, the hinging of one element and its triggered detrimental response could be properly avoided, and the system's global ductile behavior will be greatly improved. An implementation of this design idea could promote and reinforce the structural system's seismic resilience. It should be pointed that, fuse elements in realistic buildings are not necessarily placed in series, but rather could be in a complex arrangement of series or parallel.

Quantifying the strength of each fuse element such that a balanced design philosophy could be appropriately accomplished is the next step. First and foremost, one needs to identify the yield strength of each fuse separately. To simplify the mechanism, let us consider a shear wall supporting a heavy SDOF mass, and resting on a shallow footing on competent soil. Figure 3 displays two the two extreme fuse yielding mechanisms, namely the SHD and FRD systems.

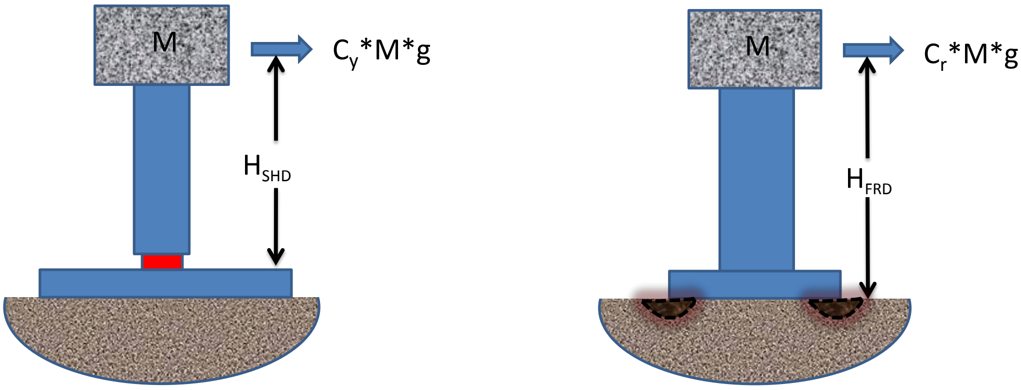

Figure 3: Schematics of SHD and FRD system.

For the structural hinging system, the moment capacity of the shear wall fuse can be correlated to the weight it must support by the following equation:

$$M_{y\_fuse} = C_y * M * g * H_{SHD} \tag{1}$$

The coefficient Cy is usually known as the base shear coefficient and in this work used to defined the yield strength associated with a structural fuse. Given the details of a shear wall, its corresponding strength can be easily computed by applying flexural beam theory. For a constant supported weight, Cy is directly proportional to the strength of the shear wall fuse, therefore it serves as an index to quantify its yield strength.

Similarly, the critical bending moment required to initiate footing rocking at footing-soil interface can be also correlated to the supported mass by introducing another dimensionless parameter Cr, which we define as the foundation rocking yield coefficient. (Deng et al. [5] and Liu et al. [14])

$$M_{y\_footing} = C_r * M * g * H_{FRD} \tag{2}$$

Deriving the footing rocking capacity ($M_{y\_footing}$) requires knowledge of the foundation geometry, axial load acting on the footing and the properties of the surrounding soil (Gajan and Kutter [8], Deng et al. [5] and Liu et al. [14]).

It is evident that, for a combined structural hinging and footing rocking structural system, the difference between Cy and Cr will render the three abovementioned footing-building configurations. A significantly larger Cy or Cr will lean the system towards behaving more like either an FRD or SHD system. By setting up Cy and Cr being approximately equal, a balanced design condition can be achieved.

It should be noted that the structural configuration for realistic buildings or bridges, are usually much more complicated than the idealized SDOF system. Therefore, the determination of these two indices should not necessarily follow the equations above, and could be varied or adjusted based on the actual structural system setup (Liu et al. [14]).

3 APPLICATION AND TESTING OF FRAME-BRACED FOUNDATION-BUILDING SYSTEM

The strength of soil, and consequently the development of a foundation rocking fuse mechanism at the soil-footing interface are greatly affected by the confining stress acting on the surrounding soil. Consequently, during an experimental evaluation, reasonably modeling of confining stress is important to capture the footings behavior. The NEES[1] centrifuge facility at the University of California, Davis (UCD) has been well established and utilized in the field of geotechnical earthquake engineering for many years (Kutter [12]), and is able to accommodate the research goals affiliated with this topic.

Two large scale system-level centrifuge tests were conducted at the UCD NEES facility. The first involved testing of three different 3-dimensional low-rise (2-story) frame-braced building models. The models included an FRD, SHD, and a BD building structure founded on shallow footings. Figure 4 provides photographs of one corner of each of the assembled models, showing both the structural fuse and footing elements. As indicated in Figure 5, the models were supported on overconsolidated clay in a rigid container and spun up to 56 RPM to create a 30-g level gravitational acceleration at the ground surface. Three models were tested at different spins and different stations; however they were subjected to a similar sequence of motions. For more details regarding the model design process, construction, instrumentation, soil profile and motion protocol, one may refer to the experimental data report (Liu et al. [13]) or a recently accepted paper (Liu et al. [14]).

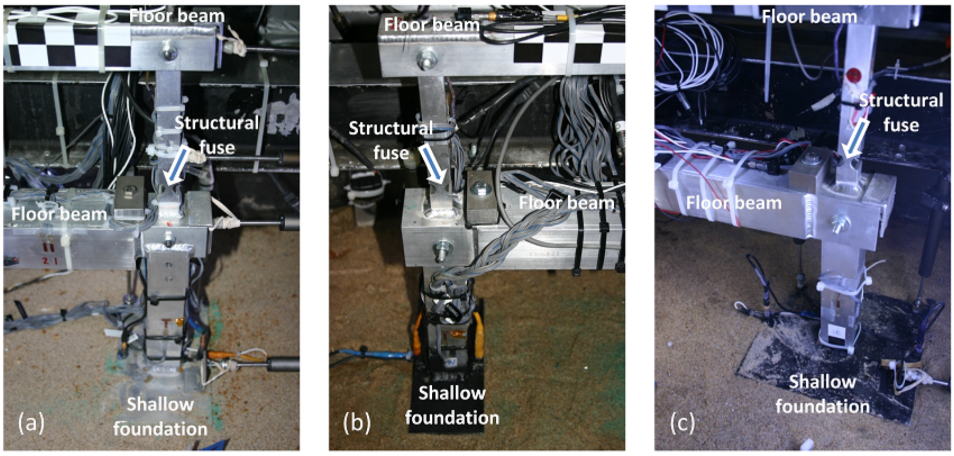

Figure 4. Photographs of: (a) BD Model; (b) FRD Model; (c) SHD Model (Liu et al. [14]).

[1] NEES is the Network for Earthquake Engineering Simulation (nees.org)

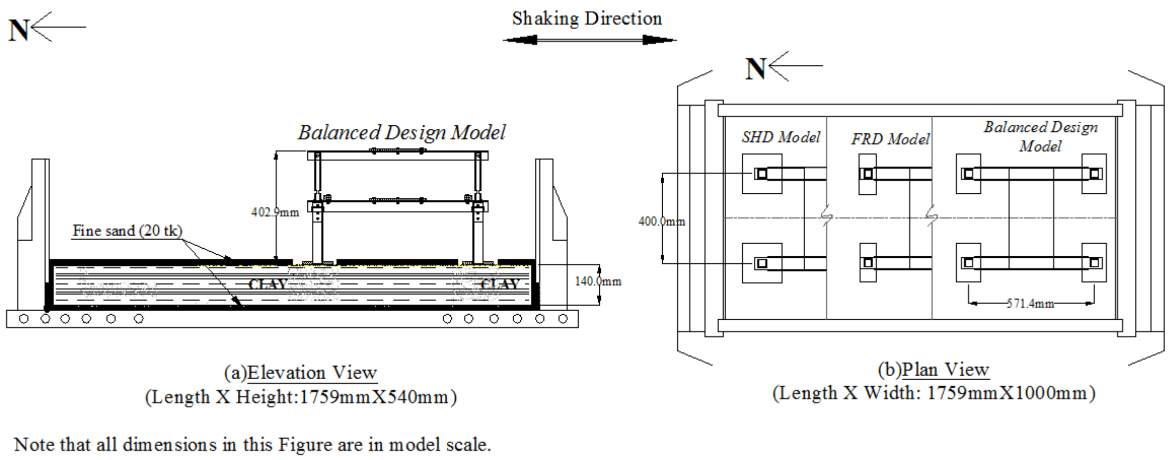

Figure 5. Model schematics and Experimental setup: (a) Elevation view; (b) Plan View.

Table 1 lists the most important system characteristics of each model, and Figure 6 shows the 5% damped elastic acceleration response spectra for each achieved input motion, overlaid with the numerically estimated first natural period of each model. Note that the intensity of the applied motion is generally gradually increased with each subsequent motion. Motions indicated by dash lines are scaled versions of recording obtained during 1971 San Fernando earthquake, while the rest plotted by solid lines are adapted from Gazli earthquake (USSR) in 1976. Unless otherwise stated, all of the results throughout this paper are expressed in prototype scale.

Parameter	Description	BD	FRD	SHD
C_r	Shallow footing rocking coefficient	0.35	0.22	0.81
C_y	Structural fuse yield coefficient	0.37	0.44	0.33
T_1 (sec)	First system natural period	0.73	0.99	0.49
T_2 (sec)	Second system natural period	0.27	0.26	0.25
FS_v	Vertical factor of safety of shallow footing	9.1	6.9	14.7
s_u	Undrained shear strength of clay		70 kPa	

Table 1: Frame-type foundation-building models' properties summary (as-built values).

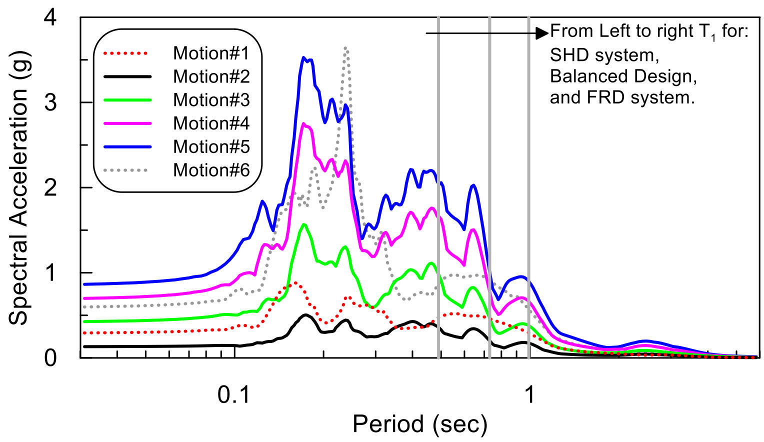

Figure 6: Input elastic spectral acceleration with 5% damping for each event.

Figure 7 displays the maximum values of selected engineering demand parameters as measured during the tests, namely the maximum roof acceleration, maximum roof drift ratio and maximum normalized base shear, for all three models. The absolute maximum roof acceleration comparison indicates that the balanced design model consistently resulted in the largest roof response. Roof acceleration is a system response and will be dictated by the strength of the foundation-building system as a whole. Total roof drift (part b) will observe contributions from both the structural fuse rotation and the footing rotation. Part (b) scatter plots reveal that the SHD system has the greatest total roof drift demand compared with the other models. In the FRD model, it has been markedly reduced in comparison with the other two models, with the exception of motion #6. Inspection of base shear coefficient indicates that system base shear demand is proportional to its footing rocking strength (Table 1). Upon moderate and intensive shaking, the SHD model is observed to have the largest base shear and the FRD has the lowest demand. Therefore, it can be concluded that implementation of relatively weaker footing element could advantageously reduce global base shear demand.

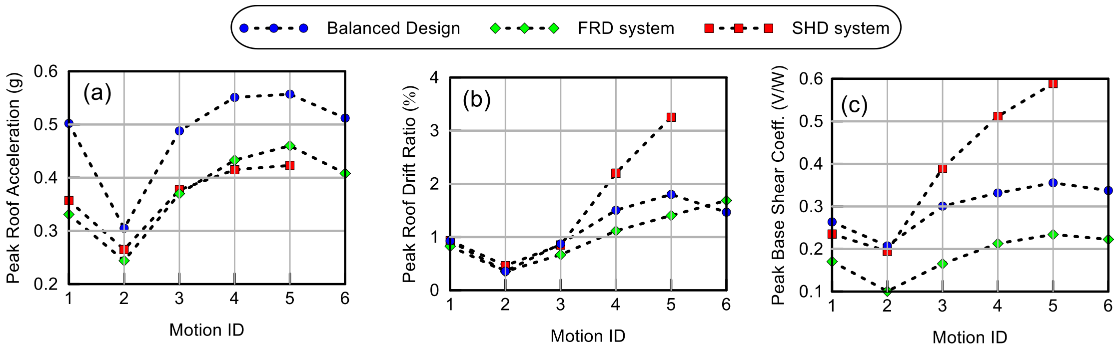

Figure 7: Selected synthesis results: (a) Peak Roof Acceleration; (b) Peak Total Roof Drift Ratio; (c) Peak Normalized Base Shear.

Figure 8 shows the dissipated energy within the fuse and footing elements, as determined using the measured moment-rotation response of the components. It is clear that the total energy is well distributed between these two elements in the balanced design configuration, irrespective of motion characteristics. For the FRD model, the foundation absorbs the majority of the input energy, which supports the fact that the structural fuse is designed to be stronger than the rocking footing element. In this case, the structural fuse behaved nearly elastically for all events. In contrast, the SHD model energy distribution is slightly sensitive to the motion amplitude and motion characteristics. Under the low amplitude motion excitation, Motion#2 for example, the foundation vibration dominates the energy absorption. While for other events, the energy is relatively well spread, but it occurred at the price of significantly higher roof drift demand, as indicated in Figure 6 (b).

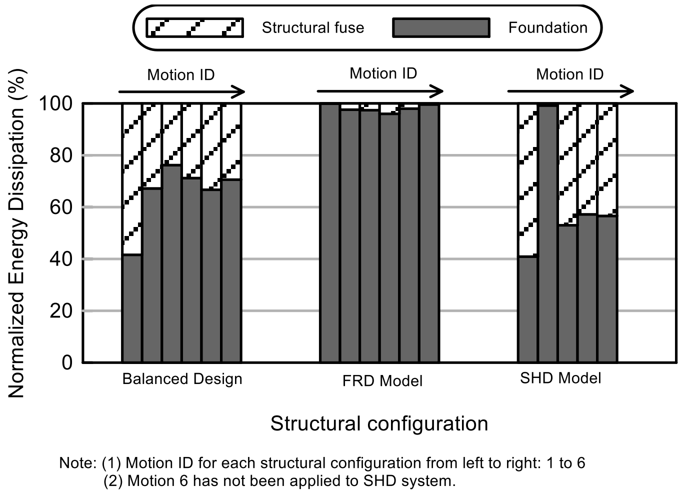

Figure 8: Normalized Energy dissipation between structural fuse and foundation element.

4 CENTRIFUGE TESTING OF WALL-BRACED FOUNDATION-BUILDING SYSTEM

The second system-level test program aims to incorporate the balanced design concept into wall-braced building system. Adopting the ASCE design guidelines (ASCE 7-10 [2]), three two-story-two-bay wall-type models were designed as planar (2-dimensional) centrifuge models. These structures represent typical low-rise segments of a building, whereby the wall component is intended to provide the majority of the lateral load resistance, yet gravity frame bays are attached and supplement not only service load carrying capacity but also inherently provide some lateral load resistance. Figure 8 shows elevation photos of each instrumented model. The simulated shear wall component was constructed by using two parallel annealed Aluminum plates (Alloy 1100-O) with a group of HDPE block spacing in between. The columns and beams were modeled by Aluminum tubing section and inverted-U channel sections, respectively. The shallow footings were designed with rectangular Aluminum block. The structural fuses were located at the base of shear wall and the ends of columns, and they were achieved via notching the edge.

Similar to the frame-braced building test objective, three different walled models were designed with a similar layout, yet with different fuse or footing geometry. In addition, the attributes of symmetry were explored by placing the wall component in the middle and at the ends of the model. This aspect is not presented in the current paper however. Parts (a) through (c) in Figure 9 displays the model of the BD, FRD and SHD building segments, respectively. Part (d) provides the overall dimensions of the models, which was consistent between the different types of structures. In addition, the sign convention adopted in subsequent plots is specified, where the (+) sign indicates that the system moves towards the exterior column and the (-) indicates movement towards the shear wall. Due to the unsymmetrical setup of the shear wall component, gravity induced load could add static moment bias at the fuse and footing level prior to dynamic shaking. This implies that shear wall fuse or footing fuse on the (+) side of the model is prone to more easily mobilize their capacity. Consequently, the response of this structural system could vary significantly in each direction, particularly when nonlinear behavior is initiated. It is desirable therefore to differentiate the direction of movement, and one should also examine the response parameters at both directions to fully understand its seismic behavior.

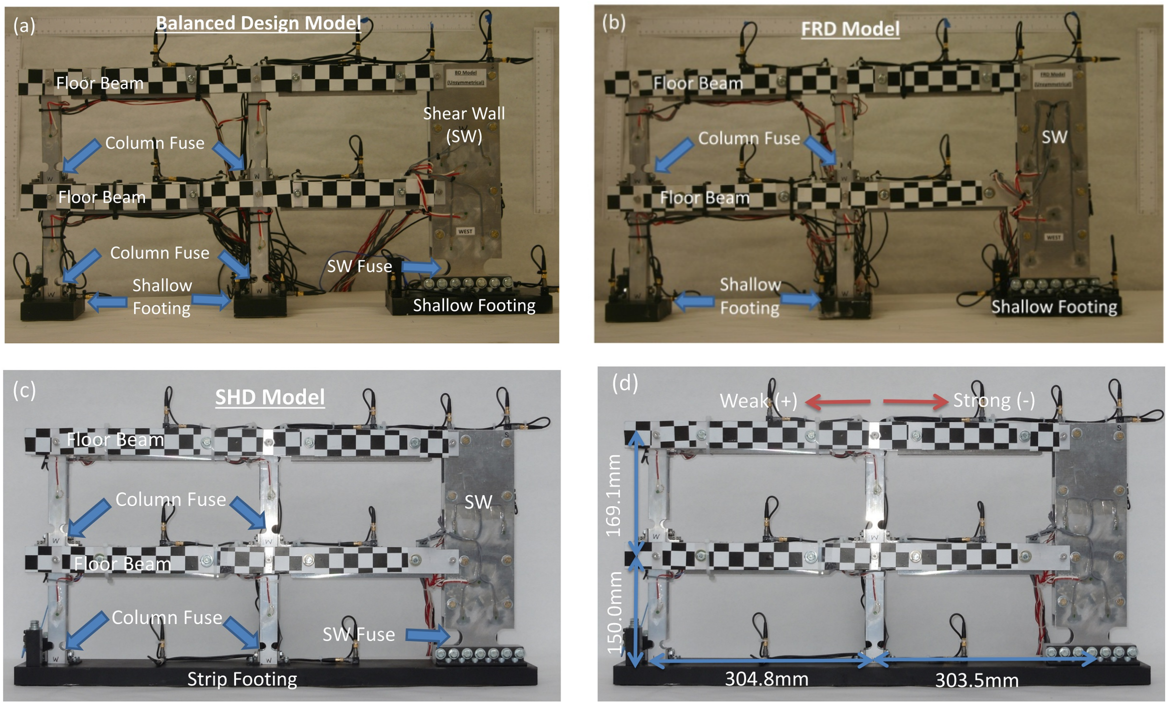

Figure 9: Elevation view of three instrumented models (a-c) and dimensional details in model scale (d).

Each model is heavily instrumented with more than 50 sensors, including accelerometers, strain gauges and linear potentiometers (Figure 9). Similar to test setup of frame models, all three wall models were supported on dry Nevada sand in a rigid container and spun up to 56 RPM to create a 30-g level gravitational acceleration at the ground surface. As indicated in Figure 10, the BD and FRD model were situated along one side of the rigid container and simultaneously subjected to a series of generally increasing amplitude motions. This arrangement could induce a more consistent input shaking for both models during the same spin. The SHD model was constructed and placed at the station where the BD had been placed following shaking of the BD and FRD model. Since the SHD model incorporates a large strip footing, any disturbance around the soil inherited from previous spins would not significantly affect its seismic response. Table 2 summarizes the most important as-built system characteristics of each model. Importantly, in contrast to the frame-braced model, the extreme cases of FRD and SHD models were able to theoretically achieve infinite Cy and Cr values when comparing with BD model.

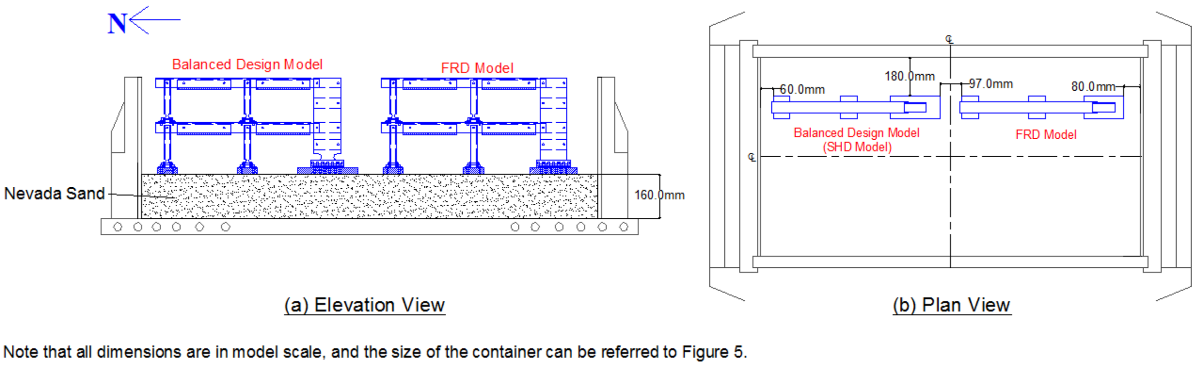

Figure 10. Experimental setup for wall-braced models: (a) Elevation view; (b) Plan view.

Parameter	Description	BD	FRD	SHD
C_r	SW footing rocking coefficient	0.24	0.16	N/A
C_y	SW fuse yield coefficient	0.29	N/A	0.29
T_1 (sec)	First natural period	0.48	0.39	0.47
FS_v	Vertical factor of safety of SW footing	20.83	17.31	N/A
$M/(V*L)$	Moment to shear ratio of SW footing	1.26	1.61	N/A
H/L	Wall aspect ratio (total height/wall length)		3.33	
D_r	Relative density of Nevada Sand		96%	
ρ	Mass density of sand		1803 kg/m^3	

Table 2: Wall-frame building model and soil properties summary (achieved values).

The three models were also subjected to an identical sequence of eleven earthquake motions. Figure 11 provides an elastic spectral acceleration response for one accelerometer located at surface free field (FF), overlaid with the estimated first natural period of each model. Table 3 lists the achieved motion characteristics of each event. The intention of the motion protocol is to employ low amplitude motions early in the series to initiate elastic response, and then gradually increase the amplitude to trigger highly nonlinear behavior towards the end.

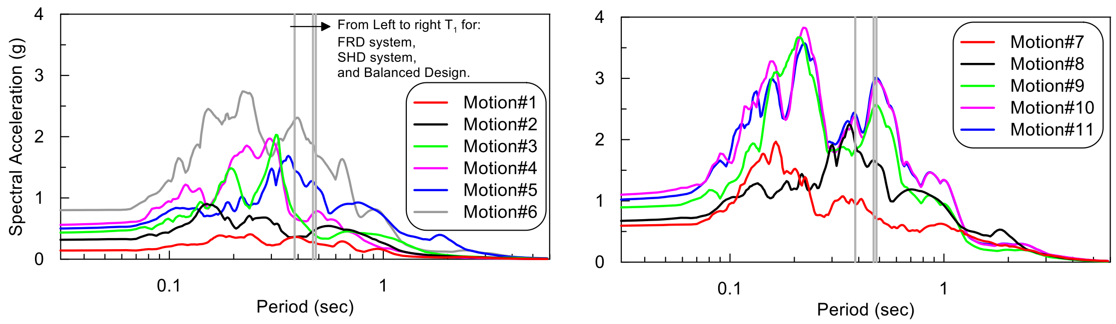

Figure 11: Elastic spectral acceleration of free field surface motion with 5% damping for all events.

Motion ID	Source Earthquake	Peak Free Field Surface Acceleration (g)	Strong Motion Duration (s)
1	Gazli, USSR, 1976	0.140	6.06
2	San Fernando, USA, 1971	0.314	6.79
3	San Fernando, USA, 1971	0.429	9.33
4	Morgan Hill, USA, 1984	0.550	3.90
5	Kobe, Japan, 1995	0.493	11.21
6	Gazli, USSR, 1976	0.797	6.06
7	Chi-Chi, Taiwan, 1999	0.586	24.11
8	Kobe, Japan, 1995	0.661	11.21
9*	Combined Morgan Step	0.882	6.86
10*	Combined Morgan Step	1.079	6.86
11*	Combined Morgan Step	1.004	6.86

*Note: these motions were an adaption of motion #4; strong motion duration is estimated by computing the time different between Arias Intensity of 95% and 5%.

Table 3: Source motion achieved characteristics.

Figure 12 compares the peak roof acceleration in (+) and (-) directions for each of the three models. The scatter plot shows that the SHD model was consistently reporting the highest roof acceleration in both the weak and strong directions, when compared with the models with footings more prone to rock. The response difference is particularly remarkable at high amplitude motions. Under motion#11, for example, the peak positive acceleration observed in the SHD model is almost double that of the FRD and BD models. However, comparing footing rocking promoted structures reveal that they have relatively similar performance at weak direction, and only moderately varying acceleration response in the strong direction, with the BD model reporting about 20% lower peak acceleration during the high intensity motions (motion #8 onward).

The peak acceleration difference observed in the wall-type structures completely deviate with the observations reported for the frame-braced models, as indicated in Figure 6 (a). This may be due to the fact that frame model is likely susceptible to higher mode effect and motion characteristics. Due to the pinned configuration at beam-column connection in frame models, second mode could either facilitate or counterbalance the movement of top story depending on the inelastic behavior development occurred within each fuse section. On the contrary, since the wall aspect ratio is relatively low, second mode contribution is very minimal for this wall-braced model.

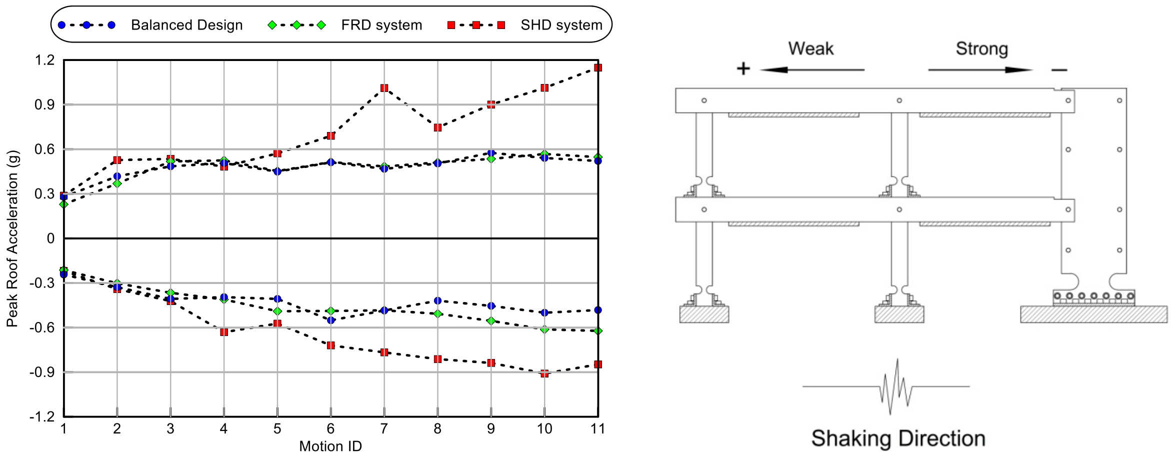

Figure 12: Peak roof acceleration comparisons at both directions.

In Figure 13, the peak roof drift demand is systematically compared among the models. The roof drift was computed by combing the high frequency component of double integration data obtained from roof accelerometer, and the low frequency component of the data recorded in LP (Deng et al. [5]). Meanwhile, this value does not account for the residual drift occurred from prior event. It is observed that the roof drift is fairly sensitive to motion characteristics. There is no definitive trend between the peak roof drift and model type for the various motions. However, comparison among the models shows that the FRD model experienced the largest roof drift, while the SHD model observes the lowest demand, and this trend is particularly pronounced in the (+) direction, i.e. towards the exterior column.

The difference in response amongst the various models also disagrees with the results generated from frame-type models. The reason for this is partially due to sectional characteristics of the dominant structural fuses, namely the column and shear wall fuses, in the frame-type and wall-type models, respectively. In the frame models, the structural fuse is dimensionally small and the entire sectional strength can be easily and fully mobilized during intense shaking, which could lead to a significant amount of sectional rotation and therefore contribute to large roof drifts of the system. On the other hand, the shear wall fuse usually develops nonlinear behavior at its extreme fiber under a rotation of about 0.5% according to a wall component test conducted following the system tests. Upon further development, strain hardening behavior combined with the wider cross section in shaking direction will result in a significant overstrength behavior. This could minimize the total fuse rotation, and thereby the entire structural displacement. In the meantime, this behavior transmits the seismic demand from fuse level to the soil-footing interface since the footing rocking capacity is lower than the shear wall fuse initial strength. As a result, large amplitude footing rocking may be observed, and the total roof drift may be significantly increased.

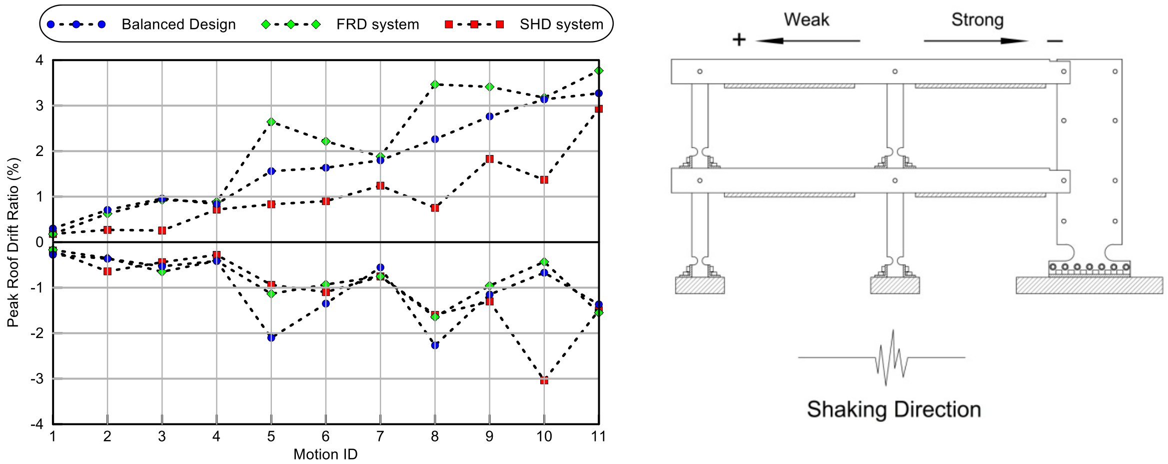

Figure 13: Peak roof drift ratio comparison at both directions.

Figure 14 plots the peak base shear demand normalized by the weight of each model (W). Similar with frame models' results, the SHD model has the largest base shear demand, regardless of motion characteristics and amplitude among the three tested models. When footing rocking is facilitated, this demand is greatly reduced as seen for the BD and FRD system. In addition, the peak base shear measured in the FRD model is less than that of balanced design. Combined with Figure 7(c), these results uniformly confirm that base shear demand is proportional to shear wall footing rocking strength. It is also notable for SHD model that the base shear demand continues to increase at high amplitude motion case despite the fact that the fuses in wall and columns have yielded at moderate motion excitation. This is directly attributed to the overstrength of the shear wall fuse.

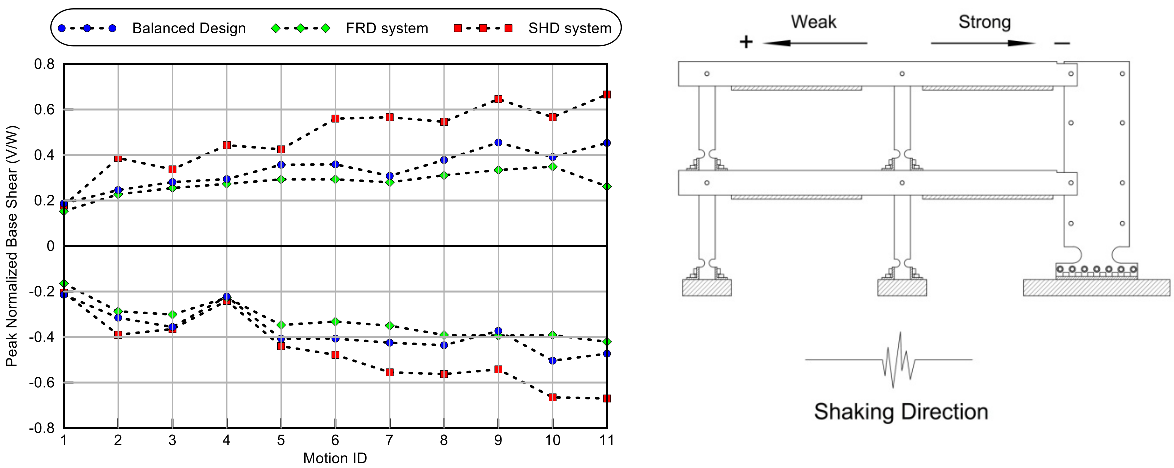

Figure 14: Peak base shear comparison at both directions.

Figure 15 documents the moment demand developed in the SW fuse and SW footing. Those demands were directly measured from the calibrated moment strain gauges. Values in the plot are the peak transient demand during shaking without considering the static load induced demand. Those values have been normalized by the respective components strength at yield (M_y). In general, the SW fuse in the SHD system experienced larger moment demands compared with the BD model. It is noted that values in excess of unity are observed around motion #4. In motion#11, for instance, the SW fuse flexural overstrength ratio reaches above 2.0 for both directions. For the SW fuse this is attributed mostly to material overstrength, whereas for the SW footing this is attributed mostly to dynamically varying axial loads, both of which modify the yield moment of the component. From motion#6 onward, the SW fuse demand in the SHD model consistently exceeds 60% of its yield strength. With footing rocking implemented (BD model), the demand to the SW fuse is reduced by at least 50%, as indicated in the blue dot line in part (a). Comparing the moment demand in the (+) and (-) directions reveals that the demand in the strong direction is larger than that of weak direction. This is due to a static moment bias in the weak direction induced by an unsymmetrical gravity load distribution.

Comparison of the footing moment demand shows that the footings of both systems likely mobilized at motion#4, and experienced an increase in moment demand upon continuing shaking. In the weak direction, the peak moment demand is about 20% greater than the theoretical yield strength at high amplitude motions. The overstrength is consistently larger in the strong direction of the shear wall, approaching 60% overstrength for each of the BD and FRD models during motion #10. Comparing the peak moment demand developed in the SW fuse and footing within the BD model indicates that the rocking foundation carries slightly more normalized moment than the shear wall fuse.

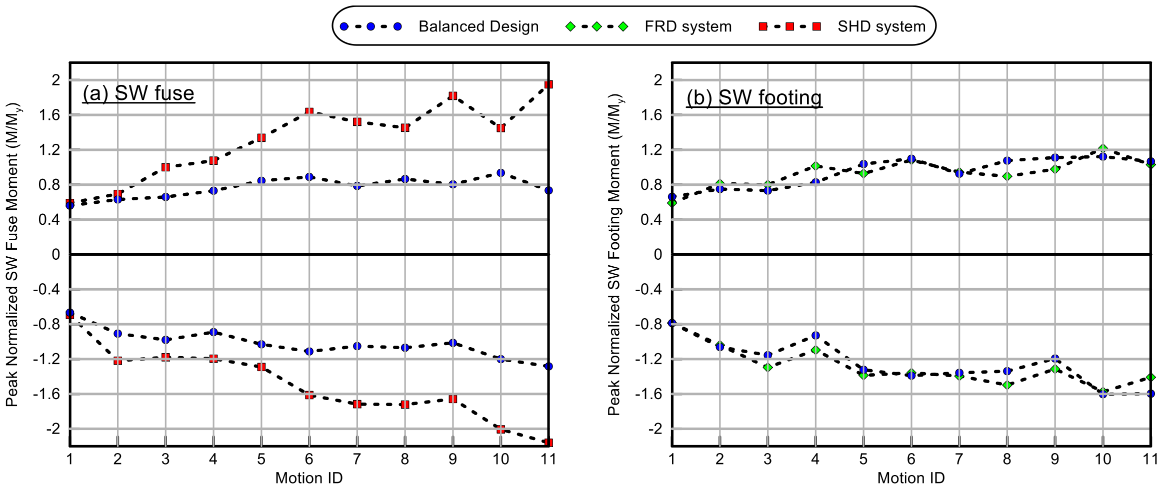

Figure 15: Peak transient moment demand comparison.

5 CONCLUSIONS

In this paper, we consider the idea of equating the rotational strength of a rocking foundation with that of conventional structural fuses and adapting this within the seismic design of a building. Three simple types of models for each of frame-braced and wall-braced types of load resisting systems used in buildings are constructed to investigate the ramification of introducing the rocking foundation as a load sharing mechanism. Models are tested at centrifuge scale considering (i) the rocking foundation and structural fuses to yield approximately simultaneously (*balanced design – BD model*), (ii) promoting only structural fuses to yield (*struc-*

tural hinging dominated – SHD model), and (iii) promoting only the foundation to yield in a mode of rocking (*foundation rocking dominated – FRD model*). Preliminary analysis of the experimental data indicates the following:

- In the frame-type building system, the balanced design model carried the largest roof acceleration compared with the FRD and SHD model. The SHD model consistently experienced the largest peak roof drift and base shear demand, while each of these responses were greatly reduced in the FRD system. In the balanced design model, the seismic energy energy dissipation was distributed between the structural fuse and rocking footing and this feature is independent of motion characteristics.

- In the unsymmetrical wall-braced systems, the SHD system has the largest peak roof acceleration demand in both the weak and strong directions, compared with the BD and FRD systems. The BD and FRD model produced a similar peak acceleration response in the weak direction. The peak roof drift is observed to be very sensitive to footing rocking. Among the three models, the FRD model consistently produced the largest total peak roof displacement. On the other hand, the SHD model reported the largest base shear force demand at the foundation level. The SW fuse in the SHD model reported large peak normalized moments, more than 50% greater than the BD model during moderate and high amplitude motions. Footings in the FRD and BD model responded with relatively consistent peak normalized moment amplitudes irrespective of the motion. Flexural overstrength is observed in both the structural fuse and rocking footing elements.

6 ACKNOWLEDGEMENTS

The research work described herein is supported by the National Science Foundation NEESR program under the award CMMI-0936503. Any opinions, findings, and conclusions expressed are those of the authors, and do not necessarily reflect those of the sponsoring organization. Special thanks go to Professor Mark Aschheim at Santa Clara University and Professor Sashi Kunnath at the University of California at Davis for their valuable suggestions and feedback during model construction and testing. Student assistants, Lijun Deng, Danielle Locklar, Kaijie Huang and Mark Stringer helped through this test program. Staff member at the UC Davis NEES facility and UCSD Powell laboratory also contributed in the program, including but not limited to: Dr. Dan Wilson, Chad Justice, Anatoliy Ganchenko, Peter Rojas and Ray Gerhard. The above support is greatly appreciated. A.G. Gavras is also grateful for the partial support provided by the Alexander S. Onassis Foundation during his M.S studies at UC Davis.

REFERENCES

[1] Anastasopoulos, I., Gazetas, G., Loli, M., Apostolou, M., and Gerolymos, N., Soil failure can be used for seismic protection of structures. *Bull. Earthq. Eng.* **8**:3, 309-326, 2010.

[2] American Society of Civil Engineers, *Minimum Design Loads for Buildings and Other Structures.* ASCE/SEI 7-10 document, ASCE, Reston, VA., 2010.

[3] Barlett, P. E., Foundation rocking on a clay soil. ME thesis, University of Auckland, *School of Engineering, Report No. 154*, Auckland, New Zealand, 1976.

[4] Chang, B. J., Thomas, J. M., Raychowdhury, P., Gajan, S., Kutter, B. L. and Hutchinson, T. C., Soil-Foundation-Structure Interaction: Shallow Foundations. Centrifuge Data Re-

port for JMT02. *University of California, San Diego, Structural Systems Research Project, Report No. SSRP-07/24*, 2007.

[5] Deng, L., Kutter, B. L., Kunnath, S., Centrifuge modeling of bridge systems designed for rocking foundations. *ASCE J. Geotech. Geoenviron. Engrg.,* **138**:3, 335-344, 2012.

[6] Drosos, V., Georgarakos, T., Loli, M., Anastasopoulos, I., Zarzouras, O. and Gazetas, G., Soil-Foundation-Structure Interaction with Mobilization of Bearing Capacity: An Experimental Study on Sand. *ASCE J. Geotech. Geoenviron. Engrg.,* **138**:11, 1369-1386, 2012.

[7] Englekirk, R. E., *Seismic design of reinforced and precast concrete buildings.* Wiley, 2003.

[8] Gajan, S., and Kutter, B. L., Capacity, settlement, and energy dissipation of shallow footings subjected to rocking. *ASCE J. Geotech. Geoenviron. Engrg*., **134**:8, 1129-1141, 2008.

[9] Gelagoti, F., Kourkoulis, R., Anastasopoulos, I. and Gazetas, G., Rocking isolation of low-rise frame structures founded on isolated footings. *Eqk. Engr. and Str. Dynamics,* **41**:7, 1177-1197, 2012.

[10] Hakhamaneshi, M., Kutter, B.L., Deng, L., Hutchinson, T.C. and Liu, W., New findings from centrifuge modeling of rocking shallow foundations in clayey ground. *ASCE 2012 Geo-congress*, Oakland, CA, Mar. 25-29, 2012.

[11] Housner, G. W., The behavior of inverted pendulum structures during earthquakes. *Bull. Seismo. Soc. Am.,* **53**:2, 403-417, 1963.

[12] Kutter, B. L., Recent advances in centrifuge modeling of seismic shaking. State-of-art paper, *Proc. 3rd Intl. Conf. on Recent Advances in Geotechnical Earthquake Engineering and Soil Dynamics,* Vol. **2**, St. Louis, 927-942, 1995.

[13] Liu, W., Hakhamaneshi, M., Kutter, B. L. and Hutchinson, T. C., Compatible soil and structure yielding to improve system performance. *Centrifuge Data Report for Test Series MAH02, Report No. UCD/CGMDR-11/07*, Center for Geotechnical Modeling, University of California, Davis, 2011.

[14] Liu,W., Hutchinson,T.C., Kutter, B.L., Hakhamaneshi, M., Aschheim, M. and Kunnath, S., Demonstration of Compatible Yielding between Soil-Foundation and Superstructure Components. *Journal of Structural Engineering, ASCE,* Posted ahead of print, April, 2012.

[15] Negro P., Paolucci R., Pedretti S., Faccioli E., Large-scale soil-structure interaction experiments on sand under cyclic loading. *Proc. 12th World Conference on Earthquake Engineering,* Auckland, New Zealand, Paper#1191, 2000.

[16] Paolucci, R., Shirato, M., and Yilmaz, M. T., Seismic behavior of shallow foundations: Shaking table experiments vs numerical modeling. *Earthquake Engineering and Structural Dynamics,* **37**, 577-595, 2008.

[17] Rosebrook, K.R., and Kutter, B.L., Soil-foundation-structure interaction: Shallow foundations. *Centrifuge Data Rep. for test series KRR01, Rep. No. UCD/CGMDR-01/09,* University of California, Davis, CA, 2001.

[18] Shirato, M., Kouno, T., Asai, R., Nakani, S., Fukui, J. and Paolucci, R., Large-scale experiments on nonlinear behavior of shallow foundations subjected to large earthquakes. *Soils and Foundations,* **48**:5, 673-692, 2008.

[19] Taylor, C.A., Crewe, A.J., Shaking table tests of simple direct foundations. *Proc. 11th World Conference on Earthquake Engineering,* Acapulco, Mexico, Paper#2048, 1996.

[20] Taylor, C. P., Cote, P. A., Wallace, J. W., Design of Slender Reinforced Concrete Walls with Openings. *ACI Structural Journal.,* **95**:4, 420-433, July-August, 1998.

[21] Trombetta, N.W., Mason, H.B., Chen, Z., Hutchinson, T.C., Bray, J.D., and Kutter, B.L., Nonlinear dynamic foundation and frame structure response observed in geotechnical centrifuge experiments. *Soil Dynamics and Earthquake Engineering*, Posted ahead of print, February, 2013.

[22] Wiessing, P. R., Foundation rocking on sand. ME thesis, University of Auckland, *School of Engineering, Report No. 203,* Auckland, New Zealand, 1979.